

## Atmospheric Extinction Coefficients and Night Sky Brightness At the Xuyi Observational Station

H.-H Zhang<sup>1</sup>, X.-W. Liu<sup>1,2</sup>, H.-B. Yuan<sup>2,3</sup>, H.-B. Zhao<sup>4</sup>, J.-S. Yao<sup>4</sup>, H.-W. Zhang<sup>1</sup> and M.-S. Xiang<sup>1</sup>

<sup>1</sup> Department of Astronomy, Peking University, Beijing 100871, P. R. China;  
[x.liu@pku.edu.cn](mailto:x.liu@pku.edu.cn)

<sup>2</sup> Kavli Institute for Astronomy and Astrophysics, Peking University, Beijing 100871, P. R. China;

<sup>3</sup> LAMOST Fellow;

<sup>4</sup> Purple Mountain Observatory, CAS, Nanjing 210008, P. R. China.

**Abstract** We present measurements of the optical broadband atmospheric extinction coefficients and the night sky brightness at the Xuyi Observational Station of Purple Mountain Observatory (PMO). The measurements are based on CCD imaging data taken in the Sloan Digital Sky Survey  $g$ ,  $r$  and  $i$  bands with the Xuyi 1.04/1.20 m Schmidt Telescope for the Xuyi Schmidt Telescope Photometric Survey of the Galactic Anti-center (XSTPS-GAC), the photometric part of the Digital Sky Survey of the Galactic Anti-center (DSS-GAC). The data were collected in more than 130 winter nights from 2009 to 2011. We find that the atmospheric extinction coefficients for the  $g$ ,  $r$  and  $i$  bands are 0.70, 0.55 and 0.38 mag/airmass, respectively, based on observations taken in several photometric nights. The night sky brightness determined from images of good quality has median values of 21.7, 20.8 and 20.0 mag/arcsec<sup>2</sup> and reaches 22.1, 21.2 and 20.4 mag/arcsec<sup>2</sup> under the best observing conditions for the  $g$ ,  $r$  and  $i$  bands, respectively. The relatively large extinction coefficients compared with other good astronomical observing sites are mainly due to the relatively low elevation (i.e. 180 m) and high humidity of the Station.

**Key words:** techniques: Astronomical observing sites: atmospheric extinction coefficients, night sky brightness

### 1 INTRODUCTION

The atmospheric extinction coefficients and night sky brightness are key parameters characterizing the quality of an astronomical observational site, in addition to the seeing and the number of clear night. The  $\alpha$  is the brightness reduction of celestial objects as their light passes through the earth atmosphere. Parrao & Schuster (2003) points out that precise atmospheric extinction determinations are needed not only for stellar photometry but also for any sort of photometry, spectroscopy, spectrophotometry and imaging whenever accurate, absolute and well-calibrated photometric measurements are required for the derivation of physical parameters in the studies of galaxies, nebulae, planets, and so forth. Precise determinations of the  $\alpha$  ultimately determine the scientific value of the telescope data. The night sky brightness is caused by the scattered starlight, the airglow, zodiacal light and the artificial light pollution from the nearby cities. It is the main noise sources of ground-based astronomical observations. The night sky brightness limits the detection depth of a telescope – the lower the night sky brightness, the fainter the stars that could be detected and the more astronomical information that could be collected.

All good astronomical sites around the world have been subject to comprehensive studies of their atmospheric extinction properties and night sky brightness measurements. For example, Krisciunas et al. (1987) and Krisciunas (1990) study the Mauna-Kea site, the host of the CFHT, the Keck 1 & 2, the Subaru telescopes as well as the future Thirty Meter Telescope (TMT) under development. Burki et al. (1995) and Mattila et al. (1996) study the La Silla site, and their results are used to refer the characteristics of the Las Campanas site that hosts the Giant Magellan Telescope (GMT). Tokovinin & Travouillon (2006) models the optical atmospheric turbulence for the Cerro Pachon site where has been selected for the Large Synoptic Survey Telescope (LSST). The  $\alpha$  and night sky brightness of the La Palma, site of the Gran Telescopio Canarias (GTC) and of a number of smaller telescopes have been studied by García-Gil et al. (2010) and Benn & Ellison (1998), respectively. Patat et al. (2011) measures the  $\alpha$  of the Cerro Paranal site of the Very Large Telescopes (VLT). Parrao et al. (2003) studies the atmospheric extinction of the San Pedro Mártir (SPM) site.

In those studies above different methods of measuring the  $\alpha$  and night sky brightness have been proposed and the results are discussed in term of affecting factors such as the aerosols, the water vapor content and the airglow, zodiacal light and light pollution. Krisciunas (1990) and Krisciunas (1997) also study and confirm the effects of the solar activities on the night sky measurements. Krisciunas & Schaefer (1991) constructs a model for the brightness of moonlight and Garstang (1989) investigates the sky brightness caused by the night glows. Hogg et al. (2001) studies the atmospheric extinction of the Apache Point Observatory (APO) and describe a near real-time extinction monitor instruments that has significantly improved the photometric calibration of the Sloan Digital Sky Survey (SDSS). Burke et al. (2010) proposes a method for precise determinations of the atmospheric extinction by studying the absorption signatures of different atmospheric constituents, which might be applied for future ground-based surveys such as the LSST. Real-time and accurate measurements of the night sky atmospheric properties will be of utter importance for future ground-based surveys.

The Digital Sky Survey of the Galactic Anti-center (DSS-GAC; Liu et al. 2012, in preparation), is a spectroscopic and photometric survey targeting millions of stars distributed in a contiguous sky area of about 3,500 sq.deg. centered on the Galactic Anti-center. The spectroscopic component of the DSS-GAC, the Guo Shou Jing Telescope (LAMOST) Spectroscopic Survey of the Galactic Anti-center (GSJTSS-GAC) will secure optical spectra for a statistically complete sample over three million stars of all colors and spectral types, whereas its photometric component, the Xuyi Schmidt Telescope Photometric Survey of the Galactic Anti-center (XSTPS-GAC) surveys the area in the SDSS  $g$ ,  $r$  and  $i$  bands with wide field CCD using the Xuyi 1.04/1.20 m Schmidt Telescope in order to provide the spectroscopic target input catalogs for the GSJTSS-GAC. XSTPS-GAC was initiated in 2009 and completed in March 2011. In total, over 20,000 images have been collected over more than 140 nights. The survey reaches a limiting magnitude of 19 ( $10\sigma$ ) in all three bands. Approximately 100 millions stars have been detected and cataloged in  $i$  band, and approximately half the number in  $g$  band.

The Xuyi Schmidt Telescope is located on a small hill about 35 km from the Xuyi country in middle-east of China with an elevation of about 180 m above the sea level, similar to the elevation of Fowler's Gap in Australia, a potential site for a Cherenkov telescope (Hampf et al., 2011). The atmospheric extinction and night sky brightness of the Xinglong station where the LAMOST is located have been studied by Yan et al. (2000) and Liu et al. (2003), respectively. In this work, we present measurements of the atmospheric extinction coefficients and night sky brightness of the Xuyi Station using the data collected for the XSTPS-GAC. The data have been analyzed using the traditional methods. The telescope characteristics and the basic data reduction steps are briefly outlined in Section 2. Section 3 presents measurements of the atmospheric extinction coefficients. In Section 4, we describe statistical measurements of the night sky brightness and discuss potential effects of the moon phase/brightness and the contribution of the Galactic disk on the night sky brightness measurements. Finally, the conclusions follow in Section 5.

**Table 1** Fields used for extinction coefficient measurements and the results

date	field <sup>a</sup>	filter	$k_1$	$k_2$	$k_c$
2010/01/06	073824+2134	<i>g</i>	$0.70717 \pm 0.01077$	$-0.02571 \pm 0.00106$	$0.02824 \pm 0.01320$
2010/01/14	073824+2134	<i>g</i>	$0.73861 \pm 0.01271$	$-0.02760 \pm 0.00145$	$0.03436 \pm 0.00746$
	073824+2134 <sup>b</sup>	<i>g</i>	$0.64923 \pm 0.06397$	$-0.10747 \pm 0.00373$	$0.00774 \pm 0.00000$
2010/10/04	011800+3000	<i>g</i>	$0.51588 \pm 0.01714$	$-0.03288 \pm 0.00117$	$0.03595 \pm 0.01222$
	011800+3000 <sup>b</sup>	<i>g</i>	$0.60061 \pm 0.02199$	$-0.01594 \pm 0.00326$	$0.02165 \pm 0.00000$
	202600+3000	<i>g</i>	$0.76053 \pm 0.01180$	$0.00178 \pm 0.00131$	$-0.00360 \pm 0.00025$
2010/09/30	011800+3000	<i>r</i>	$0.45208 \pm 0.00773$	$-0.00749 \pm 0.00126$	$0.01167 \pm 0.00330$
2010/10/05	011800+3000	<i>r</i>	$0.64922 \pm 0.01528$	$-0.01693 \pm 0.00087$	$0.02317 \pm 0.00303$
	011800+3000 <sup>b</sup>	<i>r</i>	$0.39911 \pm 0.01269$	$0.00457 \pm 0.00154$	$-0.00870 \pm 0.00156$
	202600+3000	<i>r</i>	$0.55799 \pm 0.01338$	$-0.00035 \pm 0.00143$	$0.00874 \pm 0.00194$
2010/01/13	073824+2134	<i>i</i>	$0.38335 \pm 0.01579$	$-0.00006 \pm 0.00081$	$-0.00428 \pm 0.00068$

<sup>a</sup> This column is a string expression of the field in a hhmmss+ddmm format.<sup>b</sup> The second observation of the same field on descending path from the zenith.

## 2 OBSERVATIONS AND DATA REDUCTION

The Xuyi Schmidt Telescope is a traditional ground-based refraction-reflective telescope with a diameter of 1.04/1.20 m. It was equipped with a thinned 4096×4096 CCD camera, yielding a  $1.94^\circ \times 1.94^\circ$  effective field-of-view (FoV) at a sampling of 1.705 arcsec per pixel projected on the sky. The CCD quantum efficiency, at the cooled working temperature of  $-103.45^\circ\text{C}$ , has a peak value of 90 percent in the blue and remains above 70 percent even to wavelengths as long as 8,000 Å. The XSTPS-GAC was carried with the SDSS *g*, *r* and *i* filters. The current work presents measurements of the Xuyi atmospheric extinction coefficients and the night sky brightness in the three SDSS filters based on the images collected for the XSTPS-GAC.

The XSTPS-GAC images in total a sky area of 6,000 deg<sup>2</sup> centered on the Galactic Anti-center, from 3*h* to 9*h* in right ascension (RA) and from  $-10^\circ$  to  $+60^\circ$  in declination (DEC), plus an extension about 900 deg<sup>2</sup> area toward the M31/M33 area. The sky coverage is shown in Fig. 2. Most observations were carried out in dark or grey nights of good photometric quality. A small fraction of the observations were taken under bright lunar conditions and in those cases, the angular distances between the field centers and the Moon were kept at greater than 60 deg. An integration time of 90 sec was used for all exposure, with a readout time of approximately 43 sec in dual-channel slow readout mode. The field center stepped in RA by half the Fov (i.e. 0.97 deg.), leading to two exposures for a given point of the sky. Two stripes of scan of adjacent declinations overlapped by approximately 0.04 deg. Normally, two stripes of fields of adjacent declinations were scanned in a given night. The stripes cross the Galactic disk from the south to the north, a fact that we have found useful to quantify the effects of the bright Galactic disk on the measurement of night sky brightness. With this specific combination of integration time and scanning strategy, the movement of the telescope pointing was minimized in a given night, ensuring a maximum uniformity of the survey. To facility the global flux calibration, a few "Z" stripes of fields that straddled between the fields of "normal" stripes were also observed. Finally, in the course of the survey, in order to measure the atmospheric extinction coefficients, several photometric nights were picked out and used to carry out repeated exposures of a few pre-selected fixed fields at different zenith distances, with a time interval of half an hour.

Each raw image was bias-subtracted and flat-fielded, using a super-sky-flat (SSF) generated from all frames taken in the same filter in the same night. There is interference fringing in the *i* band images. However, the fringing pattern is found to be stable for a given night, and thus can be effectively removed by SSF fielding. Aperture and PSF photometry was then performed using a package developed by the Beijing-Arizona- Taiwan-Connecticut (BATC) Sky Survey (Fan et al., 1996; Zhou et al., 2001) based on the widely used package of DAOPHOT (Stetson, 1987). The astrometry was initially calibrated with the GSC2.0 (Bucciarelli et al., 2001) reference catalog, and then the plate distortion was corrected using

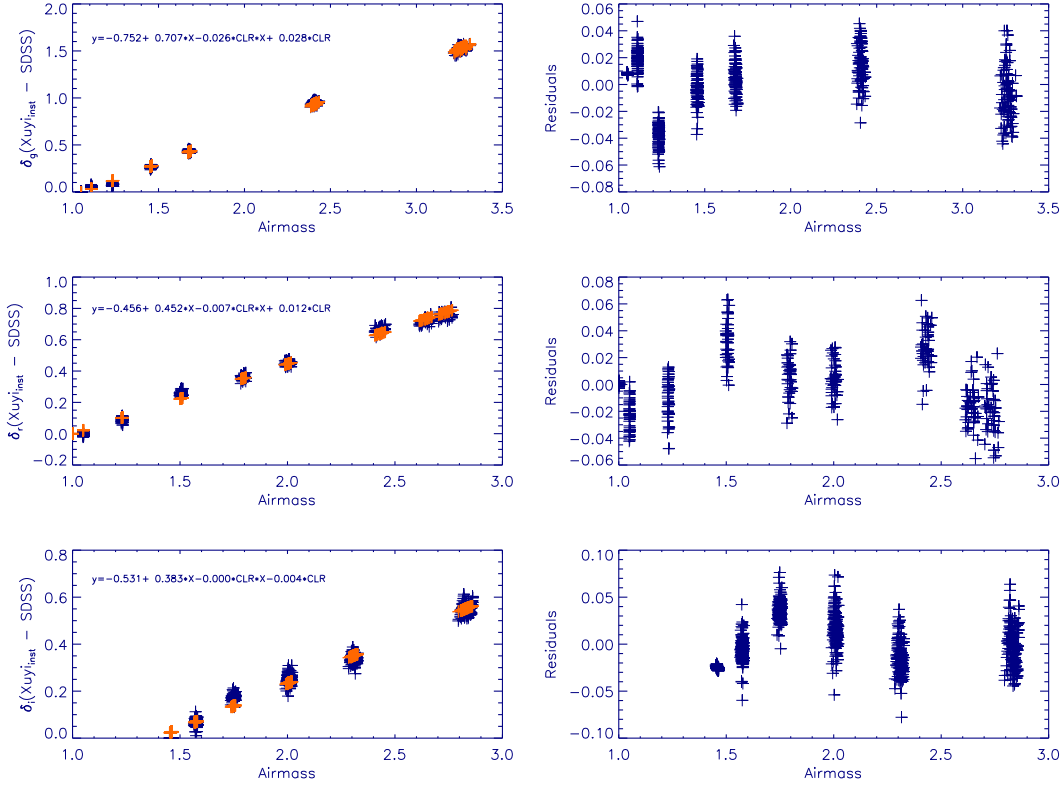


**Fig. 1** The atmospheric extinction coefficients were estimated by fitting all data points of all usable stars in a given field as is illustrated here for  $g$ ,  $r$  and  $i$  bands (from top to bottom), respectively. *Left:* The measured instrument magnitude relative to the SDSS measurements as a function of airmass, with observed values marked in blue pluses and fitted values in orange diamonds. *Right:* The fitting residuals as a function of airmass.

a 30-parameters solution based on the PPMXL (Roeser et al., 2010) reference catalogs, yielding an accuracy of about 0.1 arcsec (Zhang et al., in preparation). An UBERCAI (Padmanabhan et al., 2008) photometric calibration was achieved by calibrating against overlapping SDSS DR8 (Aihara et al., 2011) fields, yielding a global photometric accuracy and homogeneity of 2-3 percent over the whole survey area, which could be seen in (Yuan et al., in preparation).

### 3 ATMOSPHERIC EXTINCTION COEFFICIENTS

In the course of the XSTPS-GAC survey, six photometric nights were picked out in order to measure the atmospheric extinction coefficients – three nights for the  $g$  band, two nights for the  $r$  band and one night for the  $i$  band. In each night, repeated observations were carried out for one or two pre-selected fields, at different airmass with about half hour interval between the exposures. The observed fields for individual nights are listed in Table 1. In the current observations, given the large FoV of nearly 4 sq.deg., thousands bright, non-saturated stars of high signal-to-noise ratios as well as good astrometric calculation are captured in each of the individual frame of exposure, and they can be utilized to determine the astrometric extinction coefficients. For this purpose, we need color information of individuals stars. As such, we choose our fields for atmospheric extinction measurements to overlap with SDSS stripes. The SDSS source catalogs, which go deeper than ours, then provide accurate colors for all stars utilized

in the current work. Those colors are treated as "intrinsic" outside the Earth atmosphere. However, note that there are some slight differences between the XSTPS-GAC and SDSS filters. Amongst the series of images taken for each of the field, measurements made on the one of the smallest airmass were adopted as the references.

Individual frames were scrutinized and those of poor quality were rejected. Only isolated point sources within the central 1.0 sq.deg. of the field and of good signal-to-noise ratios were selected. Specifically, we required that the stars should have SDSS  $r$  band point-spread-function (PSF) magnitudes brighter than 17.0 and photometric errors less than 0.02. In addition, the measurement uncertainties of the Xuyi photometry should also be less than 0.02 mag. The stars were then examined for potential variables. The observed magnitudes of individual stars at different values of airmass were plotted as a function of airmass, and sources possessing  $3\sigma$  outliers to a linear regression were rejected, as they were likely candidates of variable stars of large variation amplitudes.

Given the large FoV, the airmass of individual stars within the frame has to be calculated separately. In addition, the effect of the spherical Earth needs to be taken into account. The following formula of airmass given by Hardie & Ballard (1962) has been adopted:

$$X = \sec z - 0.0018167(\sec z - 1) - 0.002875(\sec z - 1)^2 - 0.0008083(\sec z - 1)^3 \quad (1)$$

where  $z$  is the zenith angle in degree. The zenith angle of individual stars can be calculated from their measured celestial coordinates, the observational UT time and date. Then the instrument magnitude of a star is linked to its "intrinsic" value at the smallest airmass by the relation,

$$m_{inst} = m_0 + k_1 X + k_2 X C + k_c C + const \quad (2)$$

where  $m_{inst}$  is the stellar instrument magnitude,  $m_0$  the instrument magnitude of the same star at the lowest airmass,  $k_1$  the primary extinction coefficient,  $k_2$  the second-order extinction coefficient that relates to the color of the star,  $k_c$  a color correction factor that accounts for the small differences between the SDSS and Xuyi filter systems,  $C$  the intrinsic color of the star which taking to be the  $(g - i)$  value as given by the SDSS photometry here, and finally  $const$  a constant reflecting the zero point drift of the photometric system.

For each observed field, at least 50 stars are usable, with values of airmass of individual exposures spanning from 1.0 to 3.0 or larger. The stars also span a wide range of color of more than 0.5 mag. Thus more than 50 equations of the form of Eq. (2) could be constructed. Instead of resolving them individually, we fit all the data by a polynomial fitting in order to estimate the three extinction coefficients,  $k_1$ ,  $k_2$  and  $k_c$ . The results from individual fields are listed in Table 1. Fig. 1 shows three examples of the fitting results and their residual distribution for each band. From Table 1, we can see that, the second extinction coefficient  $k_2$  and the color coefficient  $k_c$  shows some real variations with time and seems to be needed better constrained. The cause of the variations is probably related to the changes of observing conditions, such as the humidity, winds and so on. The primary extinction coefficients  $k_1$  deduced for all three bands are large compared to typical values of some of the best astronomical sites (Mauna Kea, La Palama etc.), probably due to the low elevation of the Xuyi site.  $k_1$  also shows large variations from night to night. It seems that  $k_1$  becomes smaller after midnight, probably reflecting the drop of temperature and the content of aerosol in the air. The average values of  $k_1$  deduced from all observations are 0.69, 0.50 and 0.38 for the  $g$ ,  $r$  and  $i$  band, respectively. The  $i$  band coefficient is less well determined as there was only one night observation available. The relatively large value of the  $i$  band coefficient again possibly reflects the fact that aerosol is the dominant source of extinction for such a low altitude site.

There are three main sources of atmospheric extinction: the Rayleigh scattering, ozone absorption and aerosol dust extinction. Bessell (1990) provides empirical formula to fit the extinction of each of the three components. The magnitudes of the Rayleigh scattering [ $K_R \propto \exp(-h_0/8)\lambda^{-4}$ ] and of the aerosol absorption [ $K_A \propto \exp(-h_0/1.5)\lambda^{-0.8}$ ] both depend on  $h_0$ , the altitude in km of the site above the sea level. The low altitude of Xuyi site is clearly the main reason for the relatively large extinction coefficients, especially that of the  $g$  band, compare to other good astronomical sites which are generally at much higher altitudes. Given the significant variations of the extinction coefficients from night to

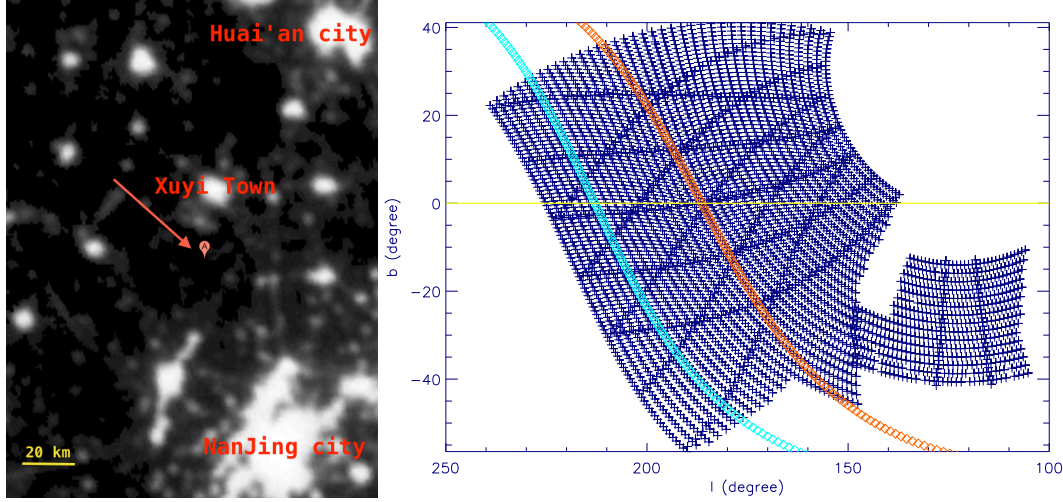


**Fig. 2** *Left:* A small portion of the map of the artificial night light from NASA's "Blue Marble" pictures (<http://www.blue-marble.de/>; 2010 version), centered on the Xuyi site marked by an arrow. The large patch of heavy light pollution near the bottom is NanJing city and the one near the top is Huai'an city are marked. The approximate range scale is labeled in the left-corner. *Right:* The sky coverage of XSTPS-GAC fields. The yellow line denotes the Galactic plane, whereas the orange diamonds denote the ecliptic and celestial equator, respectively.

night, some care must be exercised if one uses the average values presented here to reduce the whole data.

## 4 NIGHT SKY BRIGHTNESS

The sources for the night sky brightness include the diffuse stellar light scattered by the interstellar medium, the solar and lunar light scattered by atmospheric dust grains, the faint unresolved stars and galaxies within the field of view, and the scattered artificial light of cities nearby. A nice summary of the contributions of individual sources to the night sky brightness of the La Palma site is published in ?. We refer the reader to this work for details of the origins and contributions of various light sources and their potential effects on observations of different types of target. In this work we measure the night sky brightness of the Xuyi site.

### 4.1 Methods

The Xuyi site is just about a hundred kilometers away from municipal NanJing city and Huai'An city, and is about tens of kilometers away from the nearest Xuyi town. This could be seen on the map of the East Asia artificial night light picture from NASA's "Blue Marble" project (2010 version), with a small part near observation site was cut out and shown in the left panel of Fig. 2. The artificial light pollution from the nearby cities and towns are clearly visible and poses a danger to the site. In photometric nights, the light pollution is less of a problem, but in partially cloudy nights even the slightest light pollution may cause a big problem to astronomical observations due to the effects of scattering.

Only images of good quality collected in the XSTPS-GAC survey have been used to measure the night sky brightness. Images collected under cloudy conditions can be easily rejected from their abnormally bright background. To the limiting magnitude of the survey, even for crowded fields near the Galactic plane, only a small fraction of pixels are on stars and galaxies, while the rest fall on the blank sky. Thus after clipping bright pixels of stars and galaxies, the median count of blank pixels within the

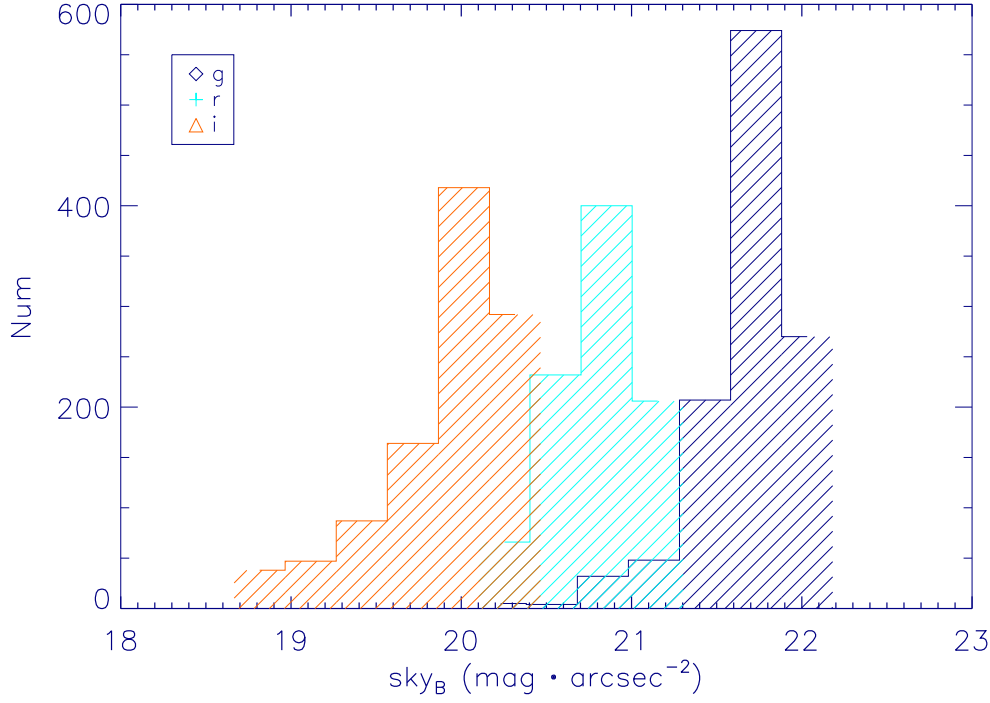


**Fig. 3** Histograms of the night sky brightness in  $g$  (blue),  $r$  (cyan) and  $i$  (orange) bands, deduced from images of Galactic latitudes  $|b| > 15^\circ$ , and taken under lunar phases  $< 7$  and angular distances  $> 90^\circ$ , more details could be seen in the text.

central  $1024 \times 1024$  CCD chip, denoted  $sky_{count}$ , serves as a robust measurement of the sky background. Then, the sky instrument brightness  $sky_{inst}$  of a given image is calculated using:

$$sky_{inst} = 25.0 - 2.5 \times \log_{10}(sky_{count}/scale^2) \quad (3)$$

where  $scale$  is the angular size of a CCD pixel projected on the sky, i.e.  $1''.705$  in this work.

Then the sky brightness  $sky_B$ , in the units of  $\text{mag}/\text{arcsec}^2$ , can be calculated by:

$$sky_B = sky_{inst} + zp \quad (4)$$

$$zp = \delta + ext + c_c \quad (5)$$

where  $zp$  is the instrument zero point,  $ext$  is the atmospheric extinction which adopted same values as deduced in previous Section,  $C_c$  is the color correction factor and  $\delta$  is the zero point for the image. Values of  $\delta$  in this work are from Yuan et al. (in preparation). Here the intrinsic night sky brightness out of the atmosphere is calculated, and we find a significant fraction of the night sky brightness at Xuyi site is from light pollution, as shown later.

## 4.2 Discussions

The right panel of Fig. 2 shows that XSTPS-GAC covers the Galactic disk and the ecliptic equator, so the data can be used to study the effects of Galactic disk and Zodiac light on the night sky brightness. Similarly, we can study the dependence of the sky brightness on the solar cycle as well as the lunar phase.

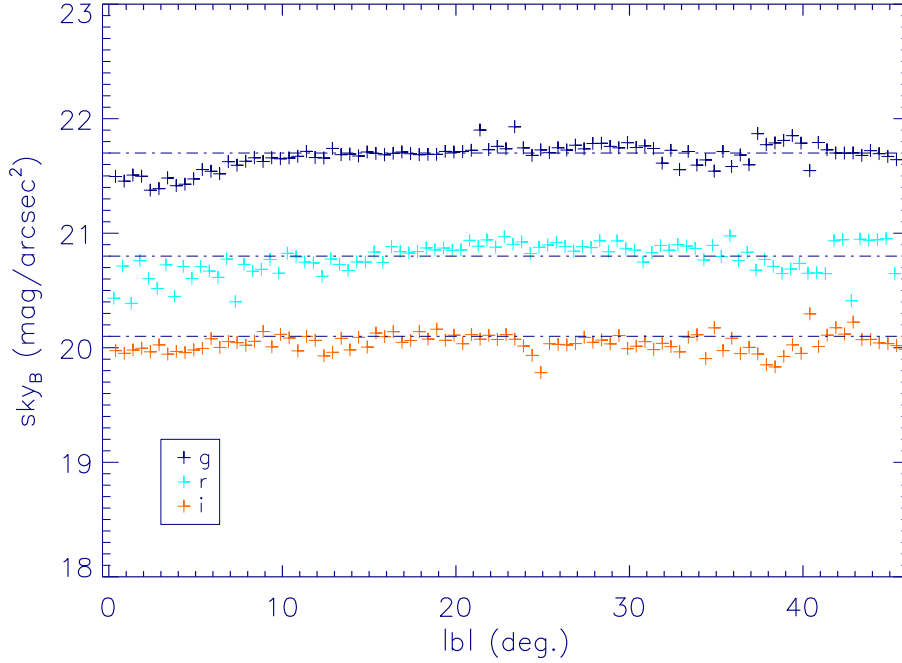


**Fig. 4** The night sky brightness variations as a function of Galactic latitude. The dot-dash lines represent the median values adopted for the Xuyi site. Each plus point represents the median sky brightness with a binsize=0.5 deg., in the units of mag/arcsec<sup>2</sup>.

The XSTPS-GAC was carried out during the early phase of the 24th solar cycle, from October 2009 to March 2012. The level of solar activity was normal and the data showed no obvious evidence that the night sky brightness was affected by the solar activities. This also implies that some caution must be exercised when comparing the night sky brightness measurements presented in the current work to other years of high levels of solar activities.

To minimize the effects of the bright Galactic disk, we calculated the night sky brightness for each band using images of ecliptic latitudes  $|\beta| > 20^\circ$ , Galactic latitudes  $|b| > 15^\circ$ , taken under lunar phases  $< 7$ , lunar angular distances  $> 90^\circ$  and lunar altitude  $< 0$  degree. Fig. 3 shows the histograms of night sky brightness distribution that were deduced for the  $g$ ,  $r$  and  $i$  band. The median values of the night sky brightness are  $g = 21.7$ ,  $r = 20.8$  and  $i = 20.0$  mag/arcsec<sup>2</sup>. Fig. 3 also shows that under best observing conditions, the night sky brightness can be as faint as 22.1, 21.2 and 20.4 mag/arcsec<sup>2</sup> in the  $g$ ,  $r$  and  $i$  band, respectively. Based on the transformation equations for population I stars between SDSS magnitudes and  $UBVR_CI_C$  given by Jordi et al. (2006)

$$V - g = (-0.573 \pm 0.002) \times (g - r) - (0.016 \pm 0.002) \quad (6)$$

and adopting  $g - r = 0.8$  as the color of the night sky, we find that a typical value of night sky brightness in  $V$  band is  $V = 21.2$  mag/arcsec<sup>2</sup>, which is very close to that of the Xinglong Station (Yao et al., 2012), but can reach to  $V = 21.6$  mag/arcsec<sup>2</sup> under best conditions. Note that the night sky brightness at the world-class sites can reach a typical value of  $V = 21.9$  mag/arcsec<sup>2</sup> (Benn & Ellison, 1998), suggesting that a significant fraction of the night sky brightness at the Xuyi site is from light pollution.

To investigate the effect of diffuse light from the Galactic disk, night sky brightness deduced from images of ecliptic latitudes  $|\beta| > 15^\circ$ , secured under lunar phases  $P < 7$ , lunar altitudes  $< 0$  and lunar angle distances  $> 90^\circ$  are plotted against Galactic latitudes in Fig. 4. Even though there are some

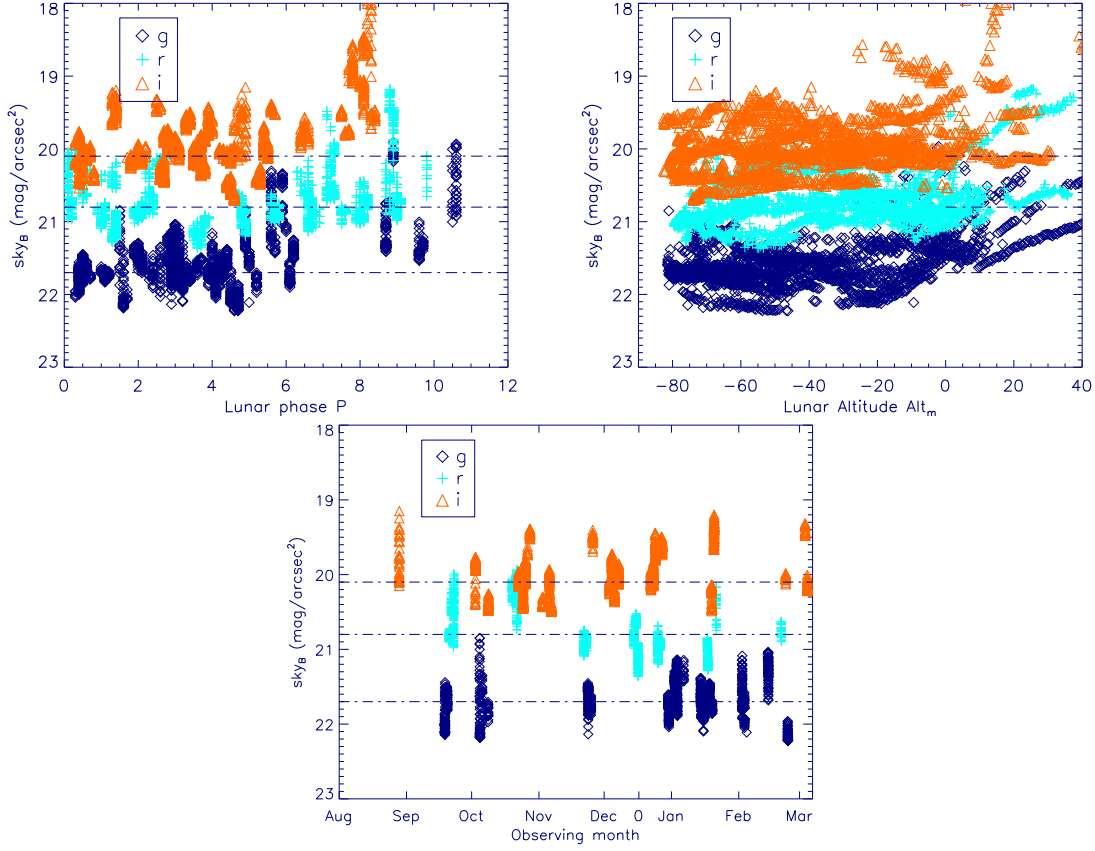


**Fig. 5** Variations of the night sky brightness with lunar phase  $P$  (top-left), altitude  $\text{alt}_m$  (top-right). In the bottom panel, only data points of  $P < 6$  and  $\text{alt}_m < 0$  are shown. The color codes of the data points are the same as in Fig. 3.

fluctuations, we can see that the Galactic disk enhances the night sky by about 0.3 and 0.2  $\text{mag/arcsec}^2$  in the  $g$  and  $r$  bands, respectively. However, the effect in the  $i$  band is not obvious. Similarly, images of Galactic latitudes  $|b| > 10^\circ$ , obtained under lunar phases  $P < 7$ , lunar altitudes  $< 0$ , and lunar angle distances  $> 90^\circ$  were used to study the variations of the night sky brightness with ecliptic latitude. No obvious variations of the night sky brightness with ecliptic latitudes are found in all the three bands.

Finally, we study the dependence of night sky brightness on the lunar phase  $P$ , lunar altitude  $\text{alt}_m$ , and the angular distance  $D$  between the field center and the Moon. A similar work on the effects of the moon on the night sky brightness is presented by Krisciunas & Schaefer (1991). The lunar phase  $P$  is normalized to 0 – 15, where 0 represents new moon and 15 full moon. Note all the observations were taken under lunar phase  $P < 10$ . Our results are shown in Fig. 5. The top left panel of Fig. 5 shows that the night sky brightness is nearly flat for  $P < 6$ , but increases significantly thereafter at a rate of about 0.3, 0.2 and 0.2  $\text{mag/arcsec}^2$  per night for the  $g$ ,  $r$  and  $i$  band, respectively. The night sky brightness is also found to be nearly constant for lunar altitudes smaller than 0 degree, i.e. below the horizon, and then brightens by about 0.2, 0.1 and 0.1  $\text{mag/arcsec}^2$  every 10 deg. for the three bands respectively as the moon rises. The bottom panel of Fig. 5 shows the seasonal variations of the night sky brightness, only images of  $P < 6$  and  $\text{alt}_m < 0$  were used. No clear seasonal variations are seen in the three bands.

## 5 CONCLUSIONS

In this work, we present measurements of the optical broadband atmospheric extinction coefficients and the night sky brightness at the PMO Xuyi site, based on the large data set collected for the DSS-GAC survey from 2009 to 2011. The mean extinction coefficients are 0.69, 0.55 and 0.38 mag/airmass for the  $g$ ,  $r$  and  $i$  band, respectively. The values are larger than the best astronomical sites, and vary from night to night. So, this result here just represents the typical atmospheric extinction for the site, it's unwise to use a single mean extinction coefficient to do the flux calibration for the whole data, which will introduce large errors.

The typical night sky brightness are 21.7, 20.8 and 20.0 mag/arcsec<sup>2</sup> in the  $g$ ,  $r$  and  $i$  band, respectively, which corresponds to  $V = 21.2$ . The night sky brightness could reach as faint as 22.1, 21.2 and 20.4 mag/arcsec<sup>2</sup> under best conditions. A significant fraction of night sky is from light pollution. The diffuse light from the Galactic disk enhances the night sky brightness by about 0.3, 0.2 and 0.2 mag/arcsec<sup>2</sup> for the  $g$ ,  $r$  and  $i$  band, respectively. But the Zodiac light has almost no obvious influences. There is no variations if lunar phase  $P < 6$  and lunar altitudes  $\text{alt}_m < 0$ . The night sky brightness will be respectively brightened by about 0.3, 0.2 and 0.2 mag per night after lunar phase  $P > 7$  and 0.02, 0.01 and 0.01 mag per degree with lunar altitudes  $\text{alt}_m$  above the horizon. The relatively faint night sky brightness makes it a good observational site in China for wide field surveys. To protect the site from further deterioration, light pollutions must be strictly controlled for any resort development around the area.

**Acknowledgements** This work is supported by the National Natural Science Foundation of China (NSFC) grant #11078006 and #10933004. And this work is also supported by the Minor Planet Foundation of Purple Mountain Observatory.

## References

- Aihara, H., Allende Prieto, C., An, D., et al. 2011, *ApJS*, 193, 29  
 Benn, C. S., & Ellison, S. L. 1998, *New Astronomy Reviews*, 42, 503  
 Bessell, M. S. 1990, *PASP*, 102, 1181  
 Bucciarelli, B., García Yus, J., Casalegno, R., et al. 2001, *A&A*, 368, 335  
 Burke, D. L., Axelrod, T., Blondin, S., et al. 2010, *ApJ*, 720, 811  
 Burki, G., Rufener, F., Burnet, M., et al. 1995, *A&AS*, 112, 383  
 Fan, X., Burstein, D., Chen, J.-S., et al. 1996, *AJ*, 112, 628  
 García-Gil, A., Muñoz-Tuñón, C., & Varela, A. M. 2010, *PASP*, 122, 1109  
 Garstang, R. H. 1989, *PASP*, 101, 306  
 Hampf, D., Rowell, G., Wild, N., et al. 2011, *Advances in Space Research*, 48, 1017  
 Hardie, R. H., & Ballard, C. M. 1962, *PASP*, 74, 242  
 Hogg, D. W., Finkbeiner, D. P., Schlegel, D. J., & Gunn, J. E. 2001, *AJ*, 122, 2129  
 Jordi, K., Grebel, E. K., & Ammon, K. 2006, *A&A*, 460, 339  
 Krisciunas, K. 1990, *PASP*, 102, 1052  
 Krisciunas, K. 1997, *PASP*, 109, 1181  
 Krisciunas, K., & Schaefer, B. E. 1991, *PASP*, 103, 1033  
 Krisciunas, K., Sinton, W., Tholen, K., et al. 1987, *PASP*, 99, 887  
 Liu, Y., Zhou, X., Sun, W.-H., et al. 2003, *PASP*, 115, 495  
 Mattila, K., Vaeisaenen, P., & Appen-Schnur, G. F. O. V. 1996, *A&AS*, 119, 153  
 Padmanabhan, N., Schlegel, D. J., Finkbeiner, D. P., et al. 2008, *ApJ*, 674, 1217  
 Parrao, L., & Schuster, W. J. 2003, in *Revista Mexicana de Astronomía y Astrofísica Conference Series*, *Revista Mexicana de Astronomía y Astrofísica*, vol. 27, vol. 19, edited by I. Cruz-Gonzalez, R. Avila, & M. Tapia, 81–89  
 Patat, F., Moehler, S., O'Brien, K., et al. 2011, *A&A*, 527, A91  
 Roeser, S., Demleitner, M., & Schilbach, E. 2010, *AJ*, 139, 2440  
 Stetson, P. B. 1987, *PASP*, 99, 191

- Tokovinin, A., & Travouillon, T. 2006, MNRAS, 365, 1235  
Yan, H., Burstein, D., Fan, X., et al. 2000, PASP, 112, 691  
Yao, S., Liu, C., Zhang, H.-T., et al. 2012, Research in Astronomy and Astrophysics, 12, 772  
Zhou, X., Jiang, Z.-J., Xue, S.-J., et al. 2001, ChJAA (Chin. J. Astron. Astrophys.), 1, 372